

Numerical Studies of the Radiant Flash Pyrolysis of Cellulose

Virendra Kothari and Michael J. Antal, Jr.*

Department of Mechanical & Aerospace Engineering
Princeton University
Princeton, New Jersey 08544

INTRODUCTION

When biomass particles are heated very rapidly ($>1000^{\circ}\text{C/s}$) in an oxygen free environment, they undergo pyrolysis with the formation of little or no char (1,2). If concentrated solar energy is used to rapidly heat the particles (3), their temperature may exceed that of the surrounding gaseous environment by several hundred degrees Celsius when pyrolysis occurs (4,5). This "two temperature" effect gives rise to the formation of high yields of sirups from the pyrolyzing biomass (6-8). Our interest in the selective formation of sirups during the radiative flash pyrolysis of biomass caused us to initiate numerical explorations of the combined effects of heat and mass transfer on the radiative flash pyrolysis phenomena. These explorations are described in this paper.

An earlier work (9) presented the derivation of the general equations governing chemical reaction, species, energy, and momentum conservation, as well as the appropriate boundary conditions, for a spherical particle of cellulose undergoing rapid pyrolysis in an intense radiative flux. The following section discusses three simplified sets of equations, which represent three different levels of physical complexity, and offer some insight into the more complex problem.

SIMPLIFIED PYROLYSIS MODELS

The general pyrolysis model (9) is specified by a coupled set of two ordinary and three partial differential equations, as well as the appropriate boundary conditions. The three "level" problems discussed in this section simplify the general problem by representing only the effects of: (1) chemical reaction and external heat transfer, (2) chemical reaction, external and internal heat transfer, and (3) chemical reaction, external heat transfer and internal mass transfer.

The major assumptions underlying the Level 1 problem are that the resistances to heat and mass transfer within the particle are negligible. Hence the particle is assumed to sustain no temperature or pressure gradients within it. We also assume that only a single vapor phase species (levoglucosan) is present within the particle, and we neglect the kinetic energy of the vapor as well as the rate of change of its enthalpy relative to that of the cellulose. Integrating over the volume of the particle, the energy conservation equation becomes

$$V_p(\rho_s c_{ps} + \rho_c c_{pc}) \frac{dT}{dt} = V_p \Delta H(-w_s) + A_p \alpha F I + A_p \bar{n}(T_f - T) + A_p \varepsilon \sigma (T_w^4 - T^4) \quad 1)$$

The reaction rate w_s is given by

$$w_s = \frac{d\rho_s}{dt} = A' e^{-E/RgT} \left(\frac{v^*}{\rho_{so}} \right)^{n-1} \rho_s^n \quad 2)$$

*Author to whom correspondence should be sent.

Present address: Department of Mechanical Engineering
University of Hawaii
Honolulu, Hawaii 96822

where

$$\rho_c = a(\rho_{so} - \rho_s) \quad 3)$$

with $\rho_{so}, \rho_c = 0$ and $T = T_i$ at $t=0$. In previous studies, a constant value for the heat transfer coefficient \bar{h} was assumed. As discussed in Reference 7, the outward bulk flow of volatiles generated by pyrolysis effectively reduces the rate at which heat is transferred from the surrounding gaseous environment to the particle. The corrected heat transfer coefficient \bar{h} is related to the uncorrected value h by

$$\frac{\bar{h}}{h} = \frac{\phi_h}{e\phi_{h-1}} \quad 4)$$

To nondimensionalize equations 1 ~ 4 we take as a reference temperature T_r the temperature at which the devolatilization rate is maximum. A reference time is chosen to be $(T_p - T_i)/\beta$ where β is a characteristic average heating rate. Table 1 summarizes the six dimensionless parameters Θ_1 - Θ_6 which result from a nondimensionalization of Eq. 1. A further discussion of the significance of these parameters is given in the following section.

The Level 2 problem accounts for the existence of temperature gradients within "large" particles undergoing rapid heating, or particles with a low thermal diffusivity. The resistance to mass transfer is still presumed to be negligible; pyrolytic vapors exit the particle without holdup. With these assumptions, the energy equation becomes

$$(\rho_s c_{ps} + \rho_c c_{pc}) \frac{\partial T}{\partial t} = \Delta H(-w_s) + \frac{1}{r^2} \frac{\partial}{\partial r} (r^2 k_e \frac{\partial T}{\partial r}) - N \frac{\partial}{\partial r} (c_p T) \quad 5)$$

wherein the molar flux of volatiles N is given by the species continuity equation

$$\frac{1}{r^2} \frac{\partial}{\partial r} (r^2 w_N) = b w_s \quad 6)$$

The initial and boundary conditions associated with Eqs. 2, 3, 5, and 6, which specify the Level 2 problem, are given by

$$\begin{aligned} t = 0 & \quad \rho_s = \rho_{so}, \rho_c = 0, T = T_i, N = 0 \\ r = 0 & \quad \frac{\partial T}{\partial r} = 0 \\ r = R & \quad k_e \frac{\partial T}{\partial r} = \alpha F I + \bar{h}(T_f - T) + \sigma e(T_w^4 - T^4) \end{aligned} \quad 7)$$

The nondimensionalization of Eqs. 2, 3, and 5-7 introduces the two new dimensionless parameters Θ_7 and Θ_8 given in Table 1.

The Level 3 problem attempts to account for the effects of mass transfer on the Level 1 problem. Two major assumptions are made: (1) the resistance to heat transfer within the particle is negligible; hence the particle is considered to be isothermal, and (2) the mass flux is given by the hydrodynamic flow expression

$$N_i = (-p_i \frac{B_o}{\mu} \frac{dc_i}{dr}) \quad 8)$$

Equation 8 presumes viscous flow to be much greater than the diffusive flow, which would be the case if the permeability B_o is large compared to the diffusivity of the gas within the solid. An evaluation of the mass transfer pecklet number $\frac{pB_o}{\mu D}$

for this problem results in a value exceeding 4000 (7), justifying assumption (2). With these assumptions, the equation governing the concentration of volatiles within the particle becomes

$$\frac{\partial}{\partial t} (\varepsilon_p c_W) - \frac{1}{r^2} \frac{\partial}{\partial r} (r^2 p W \frac{\partial c}{\partial r}) = b w_s \quad 9)$$

with $p = c R_g T$. The initial and boundary conditions are given by

$$t = 0 \quad \rho_s = \rho_{so}, \rho_c = 0, T = T_i, c = p_0 / R_g T_i$$

$$r = 0 \quad \frac{\partial T}{\partial r} = 0, \quad \frac{\partial c}{\partial r} = 0 \quad 10)$$

$$r = R \quad k_e \frac{\partial T}{\partial r} = \alpha F I + \bar{h} (T_f - T) + \epsilon \sigma (T_w^4 - T^4)$$

$$N = \bar{K} (c - c_\infty)$$

where \bar{K} is the corrected mass transfer coefficient given by

$$\frac{\bar{K}}{K} = \frac{\phi_m}{e^{\phi_m} - 1} \quad 11)$$

Thus the Level 3 problem is specified by Eqs. 1-3 and 9-11, whose nondimensionalization introduces the new parameter ϕ_m (see Table 1). The reader should note that the Level 3 problem is more mathematically complex than its predecessors due to the coupled boundary conditions in Eq. 10, reflected in the dependence of \bar{K} and K on ϕ_h and ϕ_m , which are both functions of the unknown flux of volatiles N at the surface of the particle.

RESULTS

The coupled set of ODE's and PDE's making up the Level 1-3 problems were solved using the method of lines (10) as implemented in a modified form (9) of the algorithm PDEONE developed by Sincovec and Madsen (11). The coupled system of ODE's obtained from the method of lines was integrated using the GEARB package developed by Hindmarsh (12). Numerous tests were performed to ensure the integrity (accuracy and precision) of the results, as described in detail in Reference 9.

The influence of the particle diameter, the incident intensity of solar radiation, and the freestream fluid temperature on the time dependent volatilization of the cellulose particle was studied in a variety of numerical simulations. Table 2 catalogues values of the parameters selected for study. Due to space limitations, only a small fraction of the results will be discussed here. The interested reader is referred to Reference 9 for a more complete presentation.

Figures 1 and 2 display the weight loss of a particle as a function of time (as would be measured using a TGA) for particles with diameters of 100 and 500 μm surrounded by steam at 500°C, when exposed to flux densities of 50, 100, 200, 400 and 1600 W/cm². Figure 3 shows the temperature histories of a 100 μm diameter subjected to a variety of flux densities with a freestream temperature of 800°C. It is seen that the pyrolysis of the particle can be considered to take place in two stages - a heatup stage and a devolatilization stage. In the heatup stage, the particle heats up rapidly without a significant loss of weight. As the temperature of the particle increases, the reaction rate increases considerably and the devolatilization stage sets in. As a general trend, it is observed that the time taken for complete devolatilization of the particle decreases with increasing solar flux, increasing fluid temperature and decreasing particle size. However, as evidenced in Figure 3, smaller particles subject to lower flux densities reach a stagnation temperature slightly above the freestream temperature after which little temperature change occurs until pyrolysis is complete. This causes the time for volatilization of the smaller particles subject to lower flux densities in cooler environments to increase considerably.

To calculate the values of the dimensionless numbers θ_1 - θ_6 associated with the Level 1 problem, T_p and β must be evaluated. An estimate of T_p (1) may be obtained using

$$T_p \approx E/(R_g \ln(A' R_g T_p^2 / \beta E)) \quad (12)$$

where the value β can be estimated using the following formulae for the initial values of the heating rate due to radiation and convection

$$\beta_r = \frac{4\pi R^2 \alpha F I}{\frac{4\pi R^3 \rho_{so} c_{ps0}}{3}} \quad (13)$$

$$\beta_c = \frac{4\pi R^2 h (\bar{T}_f - \bar{T}_i)}{\frac{2}{3}} / \frac{4\pi R^3 \rho_{so} c_{ps0}}{3} \quad (14)$$

with $\beta = \beta_r + \beta_c$. As discussed earlier, the value of β decreases during heatup and volatilization. This phenomena is illustrated in Figure 4. If the value of β estimated above is reduced by 50%, values for T_p estimated using Eq. 12 usually differ from the exact values by less than 50°C. Larger errors are encountered for small particles and low fluxes, when a stagnation temperature is reached. For these cases, the value $T_p = T_f$ would be more appropriate.

Tables 3 and 4 present representative values of the nondimensional numbers θ_1 - θ_6 based on values for T_p and β calculated using the above procedure. Increasing values of θ_1 and θ_2 reflect the decreasing ability of solar radiation to provide both the sensible heat and the endothermic heat of reaction requirements. The anomalous behavior of θ_3 reflects errors associated with our method for approximating the value of β used to calculate T_p . Negative values of θ_4 occur when $T_p > T_f$. For $\theta_4 < -1$ the particle should reach a stagnation temperature, in which case $T_p = T_f$ and θ_4 is artificially assigned the value $\theta_4 = 0$. As expected, values of θ_5 and θ_6 are influenced by β and T_p .

If heat transfer to the particle during devolatilization is rate limiting, then a characteristic time t_{dh} for devolatilization can be estimated using

$$t_{dh} = \frac{\Delta H \rho_{so} R}{\alpha F I + h(\bar{T}_f - \bar{T}_p)/2} \quad (15)$$

Similarly, a characteristic heatup time t_{hh} can be defined based on the sensible heat requirement:

$$t_{hh} = \frac{\rho_{so} C_{ps0} (T_p - T_i) R}{\alpha F I + h \left(\frac{(T_f - T_i) + (T_f - T_p)}{2} \right)} \quad 16)$$

Figures 5 and 6 display the relationship between the actual values for t_h and t_d and the estimated values t_{hh} and t_{dh} using Eqs. 15 and 16 above. The evident linear relationship between the estimated and actual values of t_h and t_d provides an algorithm (using Eqs. 15 and 16, and Figures 5 and 6) which accurately estimates t_h , t_d and the total time $t_t = t_h + t_d$ required for pyrolysis without resort to numerical integration of the Level 1 ODE's.

For all of the cases studied in this work $t_h < t_d$; consequently chemical kinetics control the total time required for the pyrolysis of the particle. Only for extremely high heating rates does $t_h \leq t_d$.

Figure 7 displays representative results for the Level 2 problem. In general, internal conduction and convection increase the time required for devolatilization, but have little effect on heatup. The increase in t_d is more prominent for larger particles, and higher heating rates. The fact that t_h is not dependent on internal conduction and convection may be understood in terms of the characteristic time for conduction $t_c = R^2/\alpha_s$, which takes on values 4.17, 16.7 and 417 ms for particles with diameters of 50, 100 and 500 μm (respectively). These values of t_c are comparable to the heatup times t_h for the Level 1 problem; hence the value of Θ_7 is close to unity for all the cases studied. Consequently, pyrolysis does not occur at the same time throughout the particle; rather the particle's surface rapidly heats and undergoes pyrolysis while the inside remains "cool." Thus pyrolysis occurs by ablation in all the cases studied, and t_h is unaffected by internal conduction and convection.

Table 5 displays values of Θ_8 calculated using the approximate characteristic temperature T_p defined earlier for the Level 1 problem. Values of Θ_8 indicate that for large particles and higher heating rates the internal convective heat flux (which tends to cool the particle) becomes comparable in magnitude to the conductive heat flux. This effect tends to increase t_d by counteracting heat flow into the particle during pyrolysis. Figure 8 displays the dependence of t_d (Level 2)/ t_d (Level 1) vs. Θ_8 . The observed linear dependence permits one to correct the estimated value of t_d (obtained by methods discussed earlier for the Level 1 problem) by simply evaluating Θ_8 and multiplying t_d (Level 1) by the appropriate correction factor obtained from Figure 8.

Values of Θ_9 were estimated for the range of parameters studied in this work. In almost all cases $\Theta_9 \geq 10$ (in the worst case $\Theta_9 \approx 1$); consequently for the cases studied volatiles do not accumulate within the particle and no pressure gradients are generated. For this reason, no attempt was made to solve the Level 3 problem.

CONCLUSIONS

For all the cases treated in this work, chemical kinetics control the time required to achieve devolatilization of the particle. Because of ablation, the time required for intraparticle heat transfer plays a less significant role. Mass transfer limitations were not significant for any of the cases studied.

Simple formulae were derived which facilitate rapid accurate estimates of t_h , t_d and t_t for many problems of interest. Evaluation of the nondimensional parameters $\Theta_1 - \Theta_9$ should enable other workers to apply the specific results of this work to their own problems.

Table 1
Dimensionless Parameters

Parameter	Expression	Significance
θ_1	$\frac{\rho_{ps0} c_{ps0} R_B}{\alpha F}$	sensible heat requirement heat supplied by incident solar radiation
θ_2	$\frac{\Delta H_0}{c_{ps0}(T_p - T_i)}$	heat of reaction sensible heat
θ_3	$\left(\frac{T_p - T_i}{\beta}\right) / \frac{1}{(V^*)^{n-1} A' \exp(-E/R_g T_p)}$	heatup time pyrolysis time
θ_4	$\frac{h(T_f - T_p)}{\alpha F}$	convective heat transfer incident solar radiation
θ_5	$\frac{\epsilon \sigma_w^4}{\alpha F}$	wall radiation incident solar radiation
θ_6	$\frac{\epsilon \sigma_p^4}{\alpha F}$	particle radiation incident solar radiation
θ_7	$\frac{T_p - T_i}{\beta} / \frac{R_p^2 \rho_{ps0} c_{ps0}}{k_{eo}}$	Heatup time conduction time
θ_8	$\frac{R_p^2 \rho_{ps0} V^{n-1} A' \exp(-E/R_g T_p) c_{po}}{k_{eo}} / k_{eo}$	internal convection conduction
θ_9	$\frac{P_{KB}^2}{R_g^2 T_p} / b \rho_{ps0} (V^*)^{n-1} A' \exp(-E/R_g T_p)$	volatiles flow rate volatiles generation rate

Table 2
Selected Values of Parameters
Used in the Simulations

Particle diameter = 50, 100 and 500 μ m
 Flux density = 50, 100, 200, 400 and 1600 W/cm^2
 Freestream temperature = 500° and 800°C

Table 3
Values of dimensionless parameters
100 μ diameter, $T_f = 500^\circ C$

I (W/cm^2)	θ_1	θ_2	θ_3	θ_4	θ_5	θ_6
1600	1.635	-0.0245	10.282	-0.275	0.003	0.051
400	2.041	-0.0273	10.651	-0.877	0.036	0.153
200	2.583	-0.0285	11.046	-1.598	0.072	0.274
100	3.667	-0.0510	?	?	0.144	0.144
50	5.834	-0.0510	?	?	0.283	0.288

Table 4

Values of dimensionless parameters
 500μ diameter, $T_f = 500^\circ C$

<u>I</u> <u>(W/cm²)</u>	θ1	θ2	θ3	θ4	θ5	θ6
1600	1.526	-0.0285	10.434	-0.004	0.009	0.034
400	1.607	-0.0318	11.372	-0.122	0.036	0.104
200	1.715	-0.0336	11.532	-0.210	0.072	0.182
100	1.931	-0.0354	11.451	-0.358	0.144	0.321
50	2.363	-0.0370	11.419	-0.612	0.288	0.578

Table 5

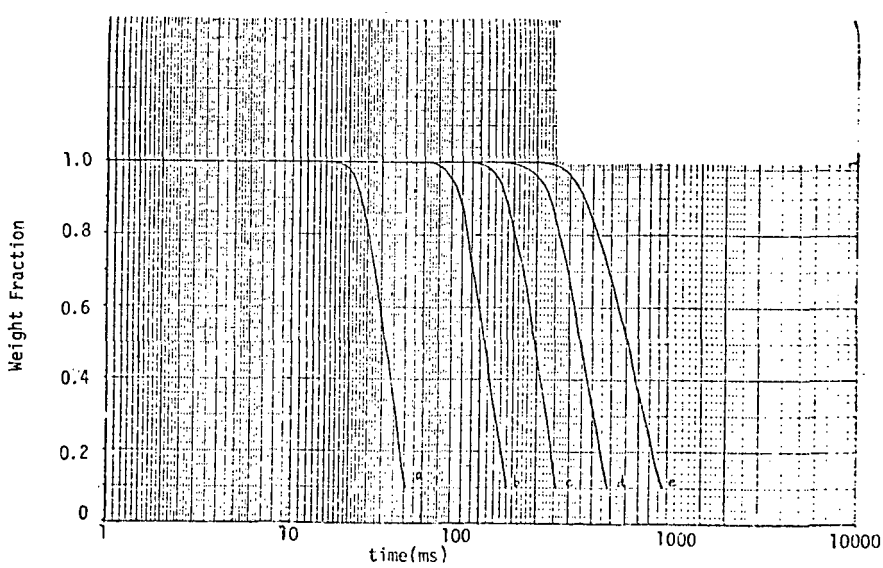
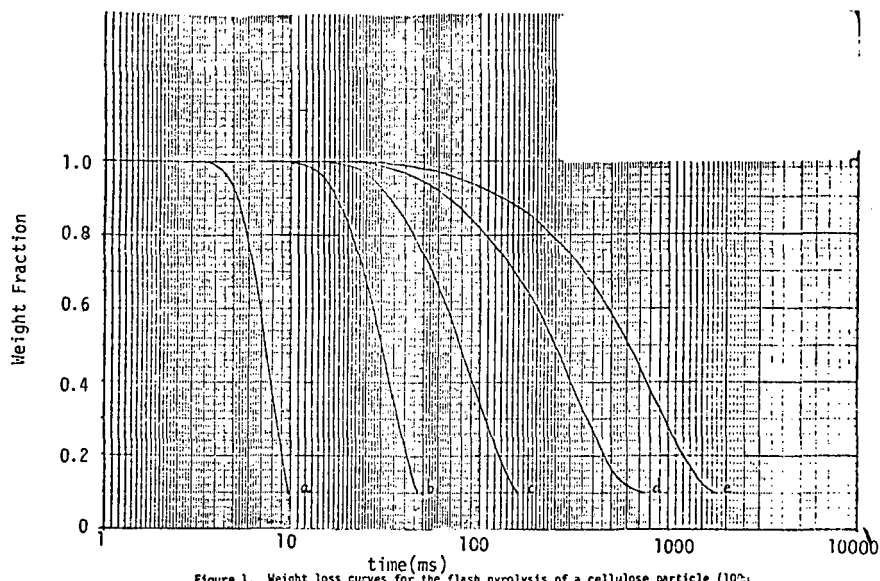
Values of the dimensionless parameter, θ_8

$T_f = 800^\circ C$

<u>I</u> <u>(W/cm²)</u>	<u>Particle diameter</u>		
	<u>50 μ</u>	<u>100 μ</u>	<u>500 μ</u>
1600	0.252	0.531	2.78
200	0.084	0.155	0.54
50	0.063	0.108	0.232

$T_f = 500^\circ C$

<u>I</u> <u>(W/cm²)</u>	<u>Particle diameter</u>		
	<u>50 μ</u>	<u>100 μ</u>	<u>500 μ</u>
1600	0.236	0.488	2.74
200		0.108	0.485
50			0.169



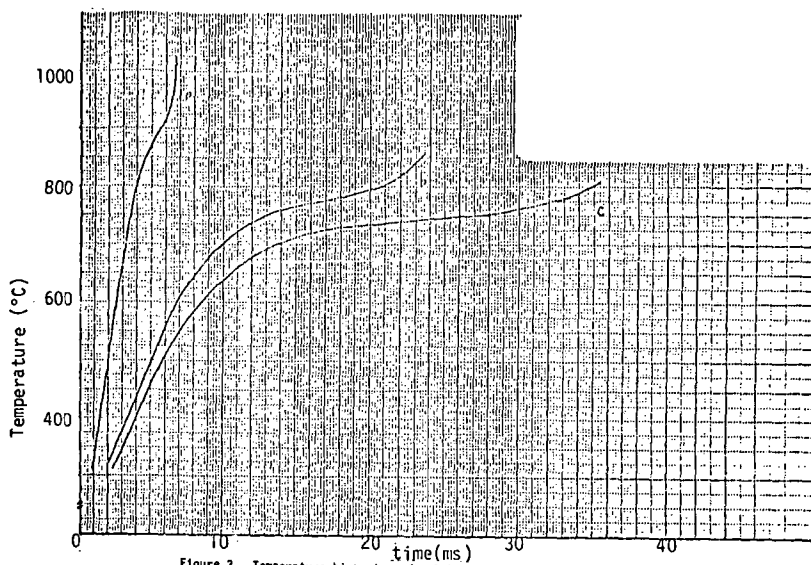


Figure 3. Temperature histories of a $100\mu\text{m}$ diameter particle at low, intermediate and high fluxes. $T_f=800^\circ\text{C}$

Curve
Flux(W/cm^2) a b c
1600 200 50

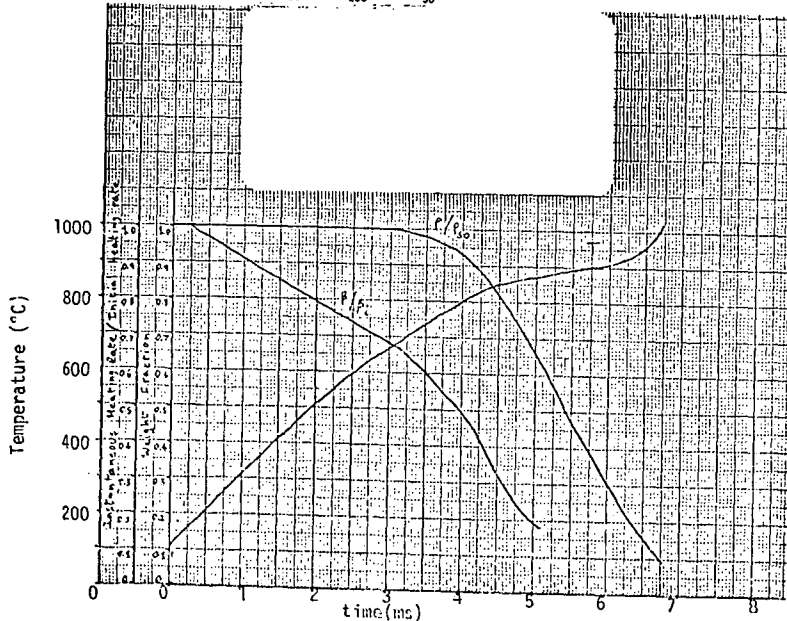


Figure 4. Weight loss, Temperature and Heating rate for a $100\mu\text{m}$ diameter particle,
 $T_f=830^\circ\text{C}$, $I=1600\text{W}/\text{cm}^2$

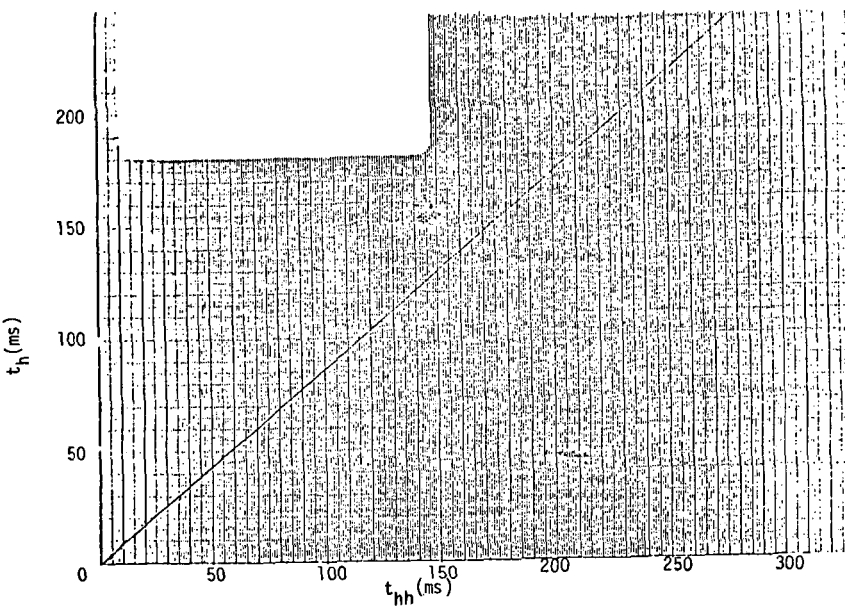


Figure 5. Plot of numerically computed heatup time, t_h , vs. characteristic heatup time, t_{hh}

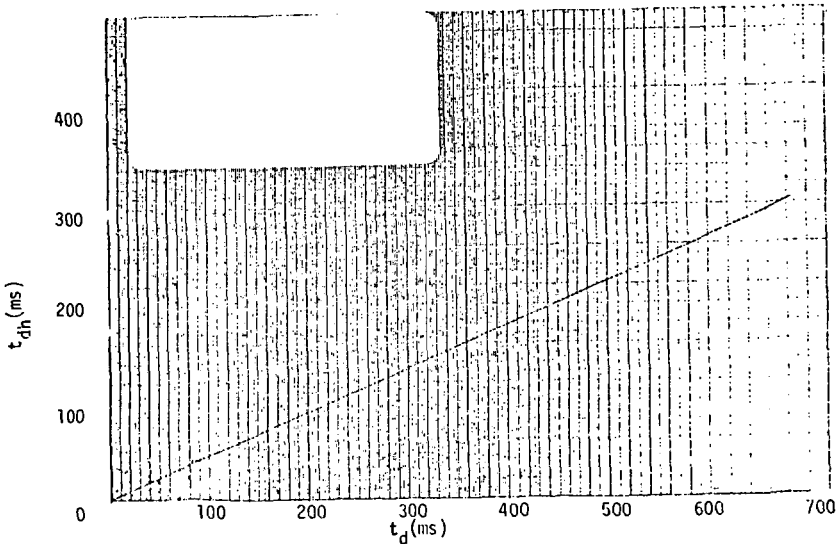


Figure 6. Plot of numerically computed devolatilization time, t_dh , vs. characteristic devolatilization time, t_{dh}

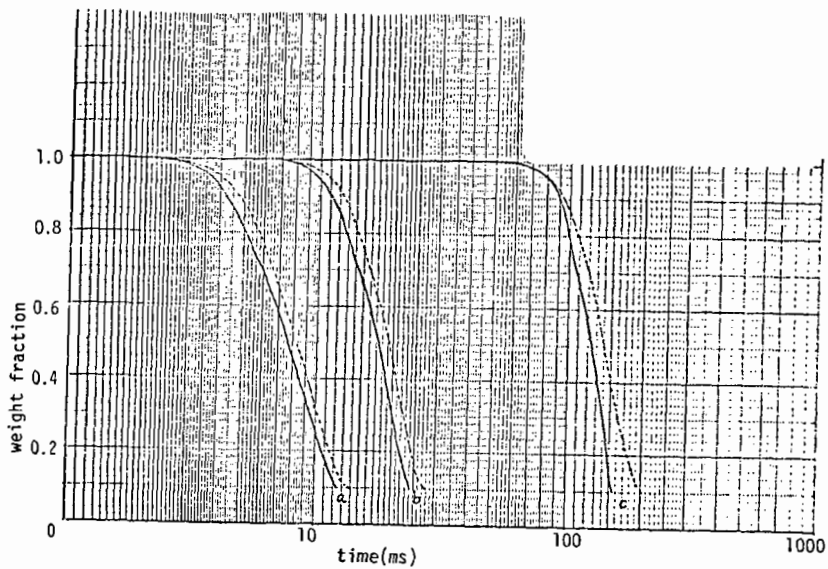


Figure 7. Plot of numerically computed heatup time, t_h , vs. characteristic heatup

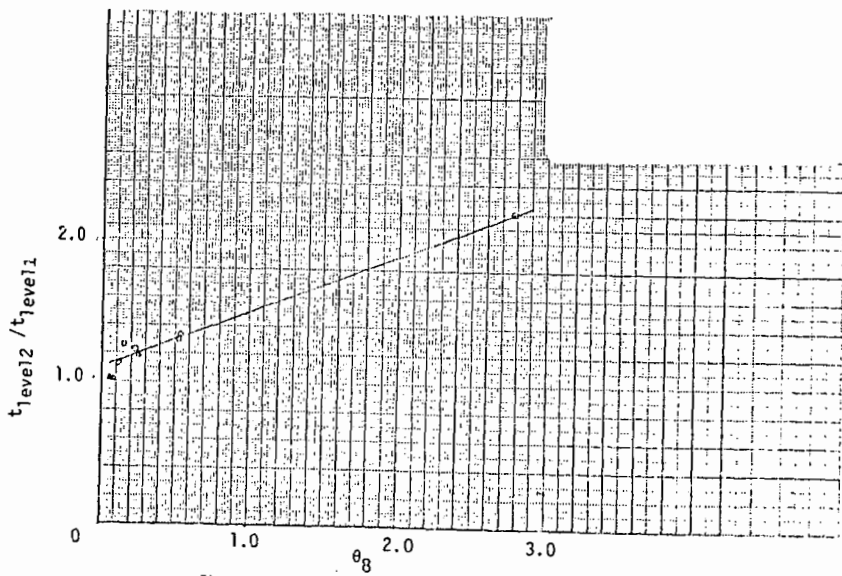


Figure 8. Plot of numerically computed devolatilization time, t_d , vs. characteristic devolatilization time, t_{dh}

REFERENCES

1. M.J. Antal, Jr. "The Effects of Residence Time, Temperature and Pressure on the Steam Gasification of Biomass" in "Biomass as a Non Fossil Fuel Source" D.E. Klass ed. A.C.S. Symposium Series No. 144, American Chemical Society, Washington, D.C. 1981 pp 313-334.
2. M.W. Hopkins, M.J. Antal, Jr., and J.G. Kay, "Radiant Flash Pyrolysis of Biomass Using a Xenon Flashtube", *J. Applied Polym. Scie.*, in press.
3. M.J. Antal, L. Hofmann, J.R. Moreira, C.T. Brown, and R. Steenblick, "Design and Operation of a Solar Fired Biomass Flash Pyrolysis Reactor", *Solar Energy*, 30, pp 299-312, 1983.
4. L. Hofmann, "Experimental and Theoretical Simulations of Solar Powered Biomass Pyrolysis Reactors", MSE thesis, Princeton University, Princeton, N.J. 1981.
5. L. Hofmann and M.J. Antal, Jr., "Numerical Simulations of Solar Fired Biomass Pyrolysis Reactors", submitted for publication in Solar Energy.
6. C.I. DeJenga, M.J. Antal and M. Jones, "Yields and Composition of Sirups Resulting from the Flash Pyrolysis of Cellulosic Materials Using Radiant Energy", *J. Applied Polym. Scie.*, 27, pp 4313-4322 (1982).
7. M.W. Hopkins, "Investigations of the Flash Pyrolysis of Biomass Using Simulated Solar Radiation", MSE thesis, Princeton University, Princeton, N.J. 1982.
8. M.W. Hopkins, C.I. DeJenga, and M.J. Antal, "The Flash Pyrolysis of Cellulosic Materials Using Concentrated Visible Light", *Solar Energy*, in press.
9. V.S. Kothari, "Numerical Studies of the Flash Pyrolysis of Cellulose", MSE thesis, Princeton University, Princeton, N.J. 1980.
10. O.A. Liskovets, "The method of Lines (review).". *Differential Equations*, 1, 1308. (English Translation). (1965).
11. R.F. Sincovec and N.K. Madsen, "Software for nonlinear partial differential equations." *ACM Trans. Math. Software* 1, 232. (1975).
12. A.C. Hindmarsh, "GEAR: Ordinary differential equation system solver." Report UCID-30001 Rev. 2, Lawrence Livermore Lab., Livermore, California. (1974).